STIC-ILL

Adams 21.50

From: Ungar, Susan
Sent: Tuesday, June 03, 2003 7:52 AM
To: STIC-ILL
Subject: Papers for Examination of SN 09234290

Hi

I need the following papers to examine 09/234,290, this is a RUSH since this case is due this biweek.

1. Yoon et al, Annals of the NY Academy of Sciences, 2001, 928:200-211

2. Poulton et al, Diabetes/Metabolism Research and Reviews, 2001, 17(6)429-435 *****

3.Hanninen et al, Immunological Reviews, 2000, 173:109-119

4. Green et al (Immunological Reviews, 1999, 169:11-22

5. Simone et al, Diabetes Care, 1999,22 Suppl 2 B7-B15

6. Palmer, J. Clin. Investigation, 2001, 108(1)31-33

7. Seddon et al (Biochem Soc. Transactions,1997, 25(2)620-624)

8. Reddy et al, Histochemical Journal, 2000, 32(4)195-206

9. Ylinen et al, Pancrea, 2000, 20(2)197-205

10. Sainio et al, Pancrea, 1999, 18(3)282-293

11. Alamunits et al, Clinical and Experimental Immunology, 1999, 115(2)260-267.

I also need an entire volume, Cohen et al (Autoimmune Disease Models, A Guidebook, Academic Press, San Diego, 1994

Thanks
Susan Ungar
1642
703-305-2181
CM1-8B05

Article title	Temporal relationship between immune cell influx and the expression of inducible nitric oxide synthase, interleukin-4 and interferon-@c in pancreatic islets of NOD mice following adoptive transfer of diabetic spleen cells
Article identifier	0018221400106231
Authors	Reddy_S Karanam_M Krissansen_G Nitschke_K Neve_J Poole_C_A Ross_J_M
Journal title	Histochemical Journal
ISSN	0018-2214
Publisher	Kluwer
Year of publication	2000
Volume	32
Issue	4
Supplement	0
Page range	195-206
Number of pages	12
User name	Adonis
Cost centre	
PCC	$21.50
Date and time	Tuesday, June 03, 2003 9:53:19 PM

The Histochemical Journal 32: 195–206, 2000.

Temporal relationship between immune cell influx and the expression of inducible nitric oxide synthase, interleukin-4 and interferon-γ in pancreatic islets of NOD mice following adoptive transfer of diabetic spleen cells

S. Reddy[1], M. Karanam[1], G. Krissansen[2], K. Nitschke[1], J. Neve[1], C.A. Poole[3] & J.M. Ross[3]
[1]*Department of Paediatrics,* [2]*Department of Molecular Medicine and* [3]*Department of Anatomy, University of Auckland School of Medicine, Private Bag 92019, Auckland, New Zealand*

Received 28 September 1999 and in revised form 20 February 2000

Summary

Beta cell destruction in NOD mice can be accelerated by adoptive transfer of diabetic spleen cells into irradiated adult NOD mice. Here mice receiving diabetic spleen cells were examined at days 0, 7, 14, 21 and at onset of diabetes for the resulting insulitis and the number of intra-islet CD4 and CD8 cells and macrophages. The progression of insulitis and the number of intra-islet CD4 and CD8 cells and macrophages were correlated with the expression and co-localization of inducible nitric oxide synthase, interferon-γ and interleukin-4 by dual-label light and confocal immunofluorescence microscopy. Diabetes developed in 7/8 mice by 27 days following cell transfer. The insulitis score increased slightly by day 7 but rose sharply at day 14 ($p = 0.001$) and was maintained until diabetes. The mean number of intra-islet CD4 and CD8 cells and macrophages showed a similar trend to the insulitis scores and were present in almost equal numbers within the islets. Immunolabelling for inducible nitric oxide synthase was observed at day 7 in only some cells of a few islets but increased sharply from day 14. It was restricted to islets with insulitis and was co-localized in selective macrophages. Weak intra-islet interleukin-4 labelling was observed at days 7 and 14 but became more pronounced at day 21 and at onset of diabetes, being present in selective CD4 cells. Intra-islet labelling for interferon-γ was first observed at day 21, but became more intense at onset of diabetes and was co-localized in a proportion of macrophages. Both cytokines were expressed in islets with advanced insulitis. Interferon-γ staining was also observed within endothelial cells located in the exocrine pancreas. We conclude that transfer of diabetic spleen cells results in a rapid influx of CD4 and CD8 cells and macrophages within the pancreas of recipient mice. During the period of heightened insulitis, selective immune cells begin to express inducible nitric oxide synthase and the opposing cytokines, interferon-γ and interleukin-4. Expression of these molecules becomes more pronounced immediately prior to and during the onset of diabetes.

Introduction

Insulin-dependent diabetes mellitus (IDDM) is an autoimmune disease and results from selective destruction of beta cells. During the disease, T cells and macrophages infiltrate the pancreatic islets progressively and mediate beta cell destruction over a prolonged asymptomatic prediabetic period (Eisenbarth *et al.* 1987, Bach 1994). The NOD mouse develops spontaneous IDDM over a protracted period also and shares many immunopathogenetic features with the human disease (Signore *et al.* 1989, Kikutani & Makino 1992). Two accelerated models of IDDM have been developed in the NOD mouse, namely the cyclophosphamide and the adoptive transfer models (Harada & Makino 1984, Wicker *et al.* 1986, Bendelac *et al.* 1987). In these models, the pancreatic islets of recipient mice are rapidly infiltrated by immune cells followed by almost synchronous development of IDDM (Kay *et al.* 1991, O'Reilly *et al.* 1991, Reddy *et al.* 1999). Thus, the accelerated models allow studies into the cellular and molecular immunopathogenesis of the disease over a narrow time frame.

In the adoptive transfer model, administration of splenocytes from diabetic NOD mice into syngeneic mice (irradiated adult NOD mice or non-irradiated newborn mice) results in accelerated diabetes (Wicker *et al.* 1986, Bendelac *et al.* 1987). Although previous studies have described the pancreatic influx of immune cells and their phenotypes in the cell transfer model, there is little information correlating the kinetics of islet invading immune cells with the expression of putative intra-islet molecular mediators of beta cell destruction. In a previous study, islets from recipient mice maintained in culture released nitric oxide (NO) in the later stages of cell transfer and at increasing levels prior to diabetes onset (Corbett *et al.* 1993). The elevated levels of NO were accompanied by a parallel and irreversible decline in glucose-induced insulin release. Recently, by *in situ* hybridization, mRNA

for tumour necrosis factor-alpha (TNF-α) and granzyme A were detected in intra-islet infiltrates of newborn mice following adoptive transfer of diabetic splenocytes (Mueller *et al.* 1995). Both, TNF-α and granzyme A, which increase the cytolytic potential of perforin expressed by CD8 cells, have been implicated in beta cell destruction in the NOD mouse (Young *et al.* 1989, Griffiths & Mueller 1991). However, the intra-islet cellular sources of these and the presence and co-localization of other putative mediators of beta cell destruction in the adoptive transfer model have not been established.

In this study, we employed the adoptive transfer model to gain further insights into the role of various intra-islet immune cells and some of the known inflammatory molecules they secrete, in beta cell destruction. Diabetic spleen cells from NOD mice were administered to irradiated adult syngeneic recipients to accelerate the disease. The resulting insulitis was quantified at different time-points following cell transfer in sections of pancreas. The progressive invasion of CD4 and CD8 cells and macrophages into the islets was enumerated following immunohistochemical staining. The insulitis scores and the kinetics of intra-islet immune cells were correlated with the expression and co-localization of inducible nitric oxide synthase, the Th1 cytokine interferon-γ, and the Th2 cytokine interleukin-4, by dual-label light and confocal microscopy.

Materials and methods

Animals

A colony of NOD/LtJ mice was established in the Animal Resources Unit of this institution from six breeding pairs originally obtained from the Jackson Laboratories, Bar Harbor, Maine, USA. The colony has been maintained under conventional conditions but with strict adherence to a high standard of hygiene. The current rate of diabetes among females is 70% between the ages of 90 and 250 days. Diabetes was defined as the presence of heavy glycosuria on three consecutive days detected by testape (Eli Lilly, St. Louis, Indianopolis, USA) and confirmed by a hyperglycemic value of > 12 mM in blood samples from the tail (Medisense blood glucose meter).

Adoptive transfer

Adoptive transfer of diabetic spleen cells was performed as reported previously (Wicker *et al.* 1986). Diabetic donor female NOD mice were killed by cervical dislocation and the spleens were removed and dispersed into single cells in Hanks Balanced Salt Solution. Spleen cell viability was determined by Trypan Blue exclusion and was found to be more than 98% viable. Splenocytes (20×10^6 cells per recipient) were injected intravenously into 8–10 week old male NOD mice which were exposed to 750 rad from a cobalt source on the previous day.

Tissue collection

Following cell transfer, pancreas was examined from groups of three recipients at days 7, 14, 21 and at onset of diabetes. Pancreas from three mice was also examined at day 0 (1 day after irradiation and without spleen cell transfer). At the appropriate time-points, animals were killed by cervical dislocation and almost the entire pancreas with a small portion of the adjacent spleen was removed, embedded in OCT and snap-frozen in isopentane precooled in liquid nitrogen. Tissues were stored at –70 °C until immunohistochemical analysis.

Pancreas from an additional three recipient mice which developed diabetes following cell transfer was fixed in Bouin's solution, processed and embedded in paraffin wax.

Primary antibodies, non-immune IgG and normal sera

Polyclonal antibodies to mouse macrophage inducible nitric oxide synthase (iNOS; rabbit IgG fraction, 1 mg/ml) were prepared by Dr. C. Nathan, Cornell University Medical College, New York, USA and supplied by Upstate Biotechnology, New York, USA. The monospecificity of this antibody for mouse iNOS has been reported previously, and it has been employed for immunohistochemical labelling of the enzyme in lipopolysaccharide (LPS) and interferon-γ (IFN-γ) activated mouse peritoneal macrophages (Xie *et al.* 1992). This antibody has subsequently been employed by the same authors for immunolocalization of iNOS in pancreatic sections of the Biobreeding (BB) rat and by us and other investigators in the NOD mouse (Kleeman *et al.* 1993, Rothe *et al.* 1994, Reddy *et al.* 1997, 1999).

Dr. H. Georgiou of the Walter and Eliza Hall Institute, Melbourne, Australia supplied rat monoclonal antibodies to mouse macrophages (MAC-1, clone M/170), CD4 (clone GK 1.5) and CD8 (clone 53-6.72) in the form of culture supernatants. The same monoclonal antibodies have been previously used for immunohistochemical staining of sections of pancreas from the NOD mouse in this laboratory (Reddy *et al.* 1995, 1997).

Rabbit polyclonal antibodies (1 mg/ml) to highly purified recombinant mouse interleukin-4 (IL-4) and mouse interferon-γ and control rabbit IgG were obtained from PeproTech Incorporated (New Jersey, USA). The control normal rabbit IgG and rabbit anti-mouse IL-4 were supplied following purification by ammonium sulphate precipitation and ion exchange chromatography while rabbit anti-IFN-γ was supplied following purification by Protein A affinity chromatography. Rat monoclonal antibodies (0.5 mg/ml, isotype: IgG_1) to highly purified recombinant mouse IL-4 (clone 11B11 and clone BVD4-1D11) and to mouse INF-γ (clone R4-6A2) and isotype matched control rat IgG_1 were purchased from Pharmingen (San Diego, California, USA). Affinity purified goat polyclonal antibodies to highly purified mouse IL-4 and mouse IFN-γ were obtained from R & D Systems, Minneapolis, MN, USA.

Rat monoclonal antibody to mouse CD31 (clone MEC 13.3, rat IgG_{2a}, κ isotype) was purchased from Pharmingen. This antibody recognizes CD31 antigen which is expressed constitutively on the surface of endothelial cells in a variety of tissues and is weakly expressed on peripheral lymphoid cells and platelets. The immunohistochemical specificity of this antibody for mouse endothelial cells has been reported previously (Vecchi *et al.* 1994).

Guinea pig anti-insulin serum was prepared by Dr. J. Crossley, Department of Paediatrics, University of Auckland and is specific for insulin (Reddy *et al.* 1988a). Rabbit polyclonal antibodies to glucagon and somatostatin were obtained from Dr. J. Livesey, Christchurch, New Zealand and Dr. J. Oliver, Adelaide, Australia, respectively, and have been employed in our previous immunohistochemical studies (Reddy *et al.* 1988b).

In the immunohistochemical procedure, all primary antisera were titrated to give maximal immunohistochemical reactivity.

Normal sera from the goat, sheep, donkey, rabbit, guinea pig, rat and mouse were available in this laboratory.

Mouse cytokines

Highly purified recombinant mouse IL-4 and IFN-γ were generously supplied by Genentech, San Francisco, USA.

Histochemical staining and evaluation of insulitis

Serial frozen sections (8 µm-thick) were prepared from different levels of the pancreas, thaw-mounted on glass slides and fixed in cold acetone for 10 min and stored at –20 °C until required. Sections from each level were stained by haematoxylin and eosin (H&E) and the islets graded for the severity of insulitis from a scale of 0–4 as reported previously (Charlton *et al.* 1988, Reddy *et al.* 1991, 1999). By this method, islets devoid of any mononuclear cells = 0, minimum focal islet infiltrate = 1+; peri-islet infiltrate of < 25% of islet circumference = 2+; peri-islet infiltration and < 50% intra-islet infiltrate = 3+; intra-islet infiltration > 50% of islet area = 4+. All slides were coded and at least 10 separate islets from different levels of the pancreas of each animal were scored. The insulitis score (%) for each study group was calculated as follows:

Sum of (1× number of islets with 1+, 2× number of islets with 2+, 3× number of islets with 3+, 4× number of islets with 4+) divided by 4× total number of islets scored. The ratio obtained was expressed as a percentage. The insulitis score (%) for each study group was expressed as the mean ± SEM.

Immunolabelling of CD4 and CD8 cells and macrophages

During the immunohistochemical procedure (described below) sections were washed in excess phosphate-buffered saline (PBS), pH 7.5, before addition of each immunological reagent. Prior to commencement of immunohistochemical labelling, sections were routinely re-fixed briefly in cold acetone, equilibrated in PBS and incubated with blocking solution (10% v/v normal sheep serum in PBS) for 30 min at 37 °C.

Immunohistochemical staining of pancreatic CD4 and CD8 cells and macrophages was carried out as described previously with minor modifications (Reddy *et al.* 1995, 1997). Following the blocking step, monoclonal antibodies to CD4 and CD8 cells and macrophages were applied to serial sections of pancreas and incubated for 2.5 h at 37 °C. After washing, sections were incubated with goat anti-rat IgG-Cy2 (1 : 50, Amersham, UK) for 1 h at 37 °C. Sections were washed and mounted with glycerol–PBS mountant and examined with an Olympus fluorescence microscope for the presence of immune cells. Selected sections were also examined by confocal microscopy.

Immune cell enumeration

The number of CD4 cells, CD8 cells or macrophages present within the islets and immediately outside the islet but in close apposition to the islet boundary were either counted microscopically or following photography as described previously (Reddy *et al.* 1995, 1999). At least 10 islets from each animal were analyzed. Results were expressed as the mean number of immune cells per islet for each group ± SEM.

Immunolabelling and co-localization of iNOS

Immunohistochemical labelling of iNOS and its co-localization in beta cells and macrophages were carried out as described recently, with minor modifications (Reddy *et al.* 1997, 1999). Following blocking with normal sheep serum, sections were incubated with anti-iNOS (1 : 200) for 16 h at room temperature followed by incubation with goat anti-rabbit IgG-biotin (1 : 200, Jackson Immunoresearch Laboratories, West Grove, Pennsylvania, USA) for 1 h at 37 °C. Sections were finally incubated with streptavidin–Texas Red (1 : 200, Jackson Immunoresearch Laboratories) for 1 h at 37 °C, washed and mounted in glycerol–PBS before microscopical examination and photomicrography.

Pairs of serial sections were also immunohistochemically stained either for beta cells or macrophages before iNOS immunolabelling. In this procedure, sections were blocked with either an equal mixture of 10% v/v normal mouse and donkey sera (for insulin staining) or 10% v/v normal sheep serum (for macrophage staining) and incubated with either guinea pig anti-insulin serum (1 : 100) or MAC-1 antibody for 2.5 h at 37 °C. They were then reacted with donkey anti-guinea pig IgG-FITC (1 : 100, Jackson Immunoresearch Laboratories) or goat anti-rat IgG cyanin-2 (1 : 50). Insulin and macrophage labelled sections were blocked with normal sheep serum and double-stained for iNOS as described above and examined by light immunofluorescence and confocal microscopy.

Immunolabelling and co-localization of cytokines

The immunohistochemical procedure adopted in this study for the cellular localization of cytokines was a minor modification of a recently reported protocol (Rothe *et al.* 1994). Preliminary results indicated that the rabbit polyclonal antibodies to IL-4 and IFN-γ showed more intense immunostaining than the corresponding rat monoclonal antibodies and goat polyclonal antibodies. Therefore, in the present study, rabbit polyclonal antibodies to the two cytokines were employed in all the immunohistochemical studies.

During the immunohistochemical procedure (described below) sections were washed in excess phosphate-buffered saline (PBS), pH 7.5 containing 0.3% saponin (Sigma, St. Louis, MO, USA). PBS–saponin also acted as the diluent for all immunological reagents for cytokine staining. Sections were re-fixed in cold acetone, equilibrated in PBS–saponin and blocked with 5% normal sheep serum for 1 h at 37 °C. After washing, they were incubated with rabbit anti-IL-4 (1 : 50) or rabbit anti-IFN-γ (1 : 50) for 18 h at 4 C. Sections were then washed and incubated with goat anti-rabbit IgG-biotin (1 : 200, Jackson Immunoresearch Laboratories) for 1 h at 37 °C. After washing, sections were incubated with streptavidin–Texas Red (1 : 200, Jackson Immunoresearch Laboratories) for 1 h at 37 °C. Sections were washed, mounted with glycerol–PBS and examined by light and confocal immunofluorescence microscopy (see below).

Groups of three serial sections were stained with anti-IL-4 or anti-IFN-γ as described above. Each of the three sections were incubated with anti-CD4, anti-CD8 or MAC-1 antibody for 2.5 h at 37 °C, washed in PBS without saponin and then incubated with sheep anti-rat IgG cyanin-2 (1 : 50) for 1 h at 37 °C. Sections were prepared for microscopical examination as described above.

Sections were immunolabelled for the two cytokines as described above and stained for insulin. Following washing, sections were blocked with normal mouse serum (20% v/v in PBS) and incubated with guinea pig anti-insulin serum (1 : 100, 1 h, 37 °C), washed and then incubated with donkey anti-guinea pig IgG-FITC (50× Jackson Immunoresearch Laboratories, 37 °C, 1 h). After the final washing, sections were prepared for microscopical examination as above.

Immunolabelling of insulin, glucagon and somatostatin

Pancreatic tissues following Bouin's fixation were employed to immunolocalize insulin, glucagon and somatostatin (Reddy *et al.* 1988a,b). Sections (5 μm) were dewaxed, hydrated and equilibrated in PBS. Following blocking with 5% normal sheep or donkey serum, sections were incubated with either guinea pig anti-insulin (1 : 50), rabbit anti-glucagon (1 : 200) or rabbit anti-somatostatin (1 : 50) for 1 h at 37 °C followed by incubation with either donkey anti-guinea pig IgG-FITC or goat anti-rabbit IgG–biotin. Sections incubated with anti-glucagon or anti-somatostatin were reacted with either streptavidin–Texas red or streptavidin–FITC. Sections immunostained for glucagon or somatostatin were also dual-labelled for insulin.

Light microscopy

Sections were examined with an Olympus UV–visible microscope equipped with excitation filters for Texas red (568 nm) and fluorescein (488 nm) and mercury and halogen lamps. At least 10 islets from each pancreas and the entire exocrine region on each slide were analyzed. Selected regions were photographed following light and confocal microscopic examination.

Confocal microscopy

Immunohistochemically-stained sections of pancreas from NOD mice were examined using a Leica TCS 4d Confocal Laser Scanning Microscope (Leica, Heidelberg, Germany) (Reddy *et al.* 1997, 1999).

The confocal system was operated in fluorescence mode to image the distribution of Texas red-labelled antigens in the section, the maximum and minimum pixel intensities being optimized for the Texas red photomultiplier channel. To image the distribution of FITC- or cyanin-2-labelled antigens, a specific FITC filter set was selected, the voltage and offset of the photomultiplier channel being adjusted to optimize pixel intensity. For the direct correlation studies, five optical sections, approximately 1 μm apart, were collected in the FITC range to image the distribution of FITC- or cyanin-2-labelled antigens. The filter set was then changed to provide a 568 nm line to excite Texas red, and a separate series of the corresponding Texas red-labelled antigen was collected through the identical z-series co-ordinates.

Each digital set was collected on the confocal microscope and processed using the 3D software included with the Leica ScanWare operating system to construct a z-series projection, a computer-averaged assembly of all optical sections in the data set. The images were saved in a TIFF file format before transfer to a Power Macintosh 7100/80 AV for image processing.

Image processing and photography

Appropriate fields from light immunofluorescent stained sections and sections following H&E staining were photographed with a Kodak Ektachrome 200 ASA film and the images transferred to a photo compact disk.

Confocal images were assembled in Adobe Photoshop 4.0 (Adobe Systems Inc, USA). The FITC distribution was assigned a fluorescent green colour and the Texas red distribution a bright red colour. Separate fluorescent images as well as merged images were saved as TIFF files.

Immunohistochemical controls

In the immunohistochemical procedure, the primary antibodies against iNOS, IL-4, IFN-γ, glucagon or somatostatin were replaced with buffer, normal rabbit IgG or normal sera

from a rabbit, mouse, rat or guinea pig at equivalent dilutions and primary and secondary steps were omitted. In the immunohistochemical procedure for IL-4 and IFN-γ, the primary rabbit antiserum was absorbed with an excess of the homologous cytokine (0.5 and 1 μg per μg anti-IL-4 or anti-IFN-γ immune IgG) prior to use. In the immunohistochemical protocol for insulin, the primary antiserum was absorbed with excess highly purified bovine insulin (1 μg insulin per μl of original immune serum) before use. It was also substituted with normal guinea pig serum. In the double staining protocol, species-specific secondary antibodies (FITC- or biotin-linked) were replaced by incompatible antibodies. Dual staining was also performed in the absence of one of the two primary antibodies.

Statistical analysis

For the insulitis scores, an arc sine transformation was used. Polynomial regression was used to investigate whether there was a difference in the change in insulitis score over time. As most islets had zero immune cell infiltration at day 0, the change in the number of immune cells was investigated from day 7 until the onset of diabetes. A square root transformation was used on the cell counts to adjust for the correlation between the mean and variance in counts. Polynomial regression was used to investigate the change in the number of CD4 and CD8 cells and macrophages over time.

Results

Incidence of diabetes following adoptive transfer

Diabetes developed in 7/8 mice between days 17 and 28 following spleen cell transfer. Among the 7 diabetic mice, a single mouse developed the disease at day 17, two at day 23 and the remaining 4 mice at day 27.

Severity of insulitis

The mean insulitis score % ± SEM at various time-points following cell transfer is shown in Figure 1. At day 0 (1 day after irradiation and without spleen cell transfer), the severity of insulitis was either negligible or absent in most islets. The insulitis score showed a moderate increase at day 7 but rose rapidly at day 14 ($p = 0.001$). This was maintained at day 21 and at onset of diabetes. Insulitis scores showed a change over time and a quadratic term was found to be significant (F 1, 15 = 6.05, $p = 0.030$).

Figure 2a–f shows representative photomicrographs of the changing pattern of immune cell influx into the islets following cell transfer.

Intra-islet CD4 and CD8 T cells and macrophages

The kinetics of intra-islet CD4 and CD8 cells and macrophages showed a similar trend to the insulitis scores until day 14 (Figure 3). All three cell-types in the intra-islet areas

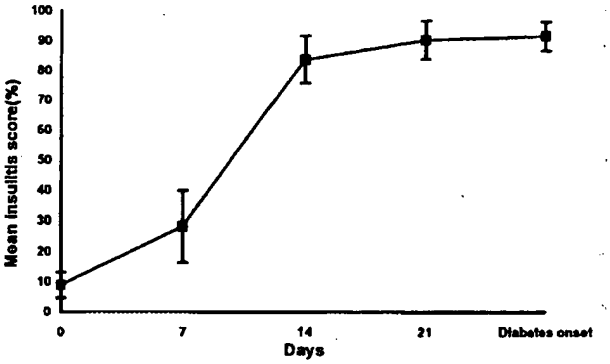

Figure 1. The mean insulitis scores (% ± SEM) in recipient mice at various time-points following administration of diabetic spleen cells. Insulitis scores were obtained from three mice at each time-point. The insulitis scores showed a statistically significant increase from day 7 to either days 14, 21 or until diabetes onset ($p = 0.001$; polynomial regression analysis) but not from days 0 to 7 or between days 14 to onset of diabetes.

showed a rapid increase from days 7 to 14 which was maintained until day 21. The mean number of intra-islet CD4 and CD8 cells declined gradually from day 21 until the onset of diabetes. The mean number of intra-islet macrophages showed a small increase from days 14 to 21 but declined at onset of diabetes. At each time-point the mean number of intra-islet immune cell-types was not significantly different.

Separate analyses for CD4 and CD8 cells and macrophages showed that there was a change in the mean number of cells per islet over time (F 2, 477 = 4.01, $p = 0.02$) and was different for the three cell-types. A quadratic curve was appropriate for all three analyses ($p < 0.0001$ in all cases). There was a significant increase in the mean number of immune cells per islet from days 7 to 14 ($p = 0.001$) followed by a slight decline from day 21 to onset of diabetes ($p = 0.01$).

From day 7 onwards CD4 and CD8 cells and macrophages were observed in exocrine regions also. Representative photomicrographs showing the intra-islet distribution of the three immune cell types at various time-points following cell transfer are shown in Figure 2g–r.

Expression of insulin, glucagon and somatostatin at onset of diabetes

At onset of diabetes, insulin immunoreactive cells were either reduced or absent (Figure 4a–c). In contrast, glucagon and somatostatin cells were preserved in several infiltrated islets and in atrophied islets devoid of immune cells (Figure 4a,c). The distribution of glucagon cells as a dense core within an atrophied islet is shown in Figure 4c.

Expression and co-localization of iNOS

Following administration of diabetic splenocytes, immunolabelling of iNOS was first observed at day 7 in a small proportion of islets (Figure 4d). At days 14 and 21 and at onset of diabetes, weak, moderate and intense immunolabelling of

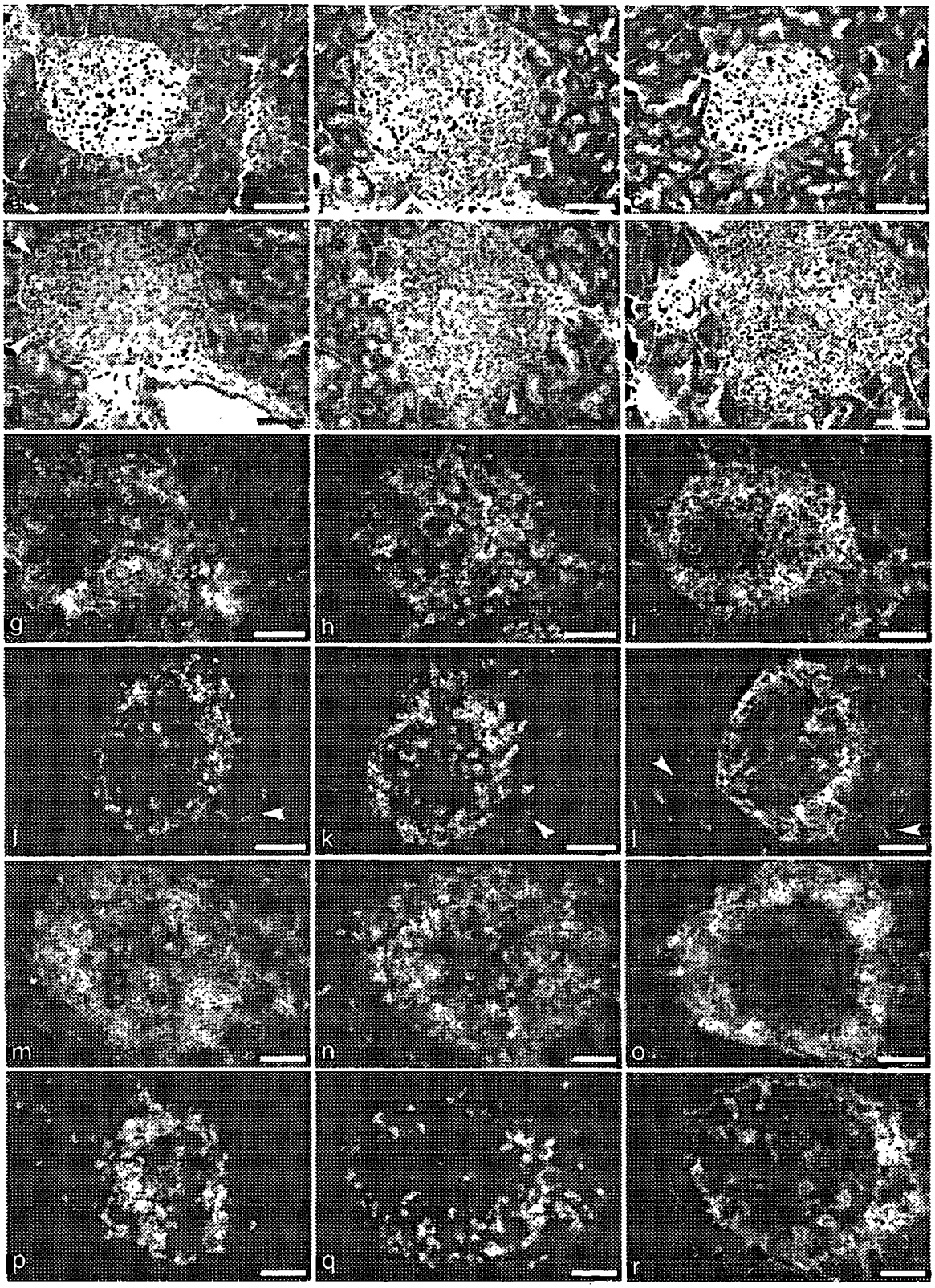

Figure 2. (a–f): Representative photomicrographs of H&E-stained pancreatic sections from recipient mice showing insulitis at various time-points following administration of diabetic spleen cells. (a): Day 0: a large and a small islet without insulitis. (b,c): Day 7: an islet in (b) with

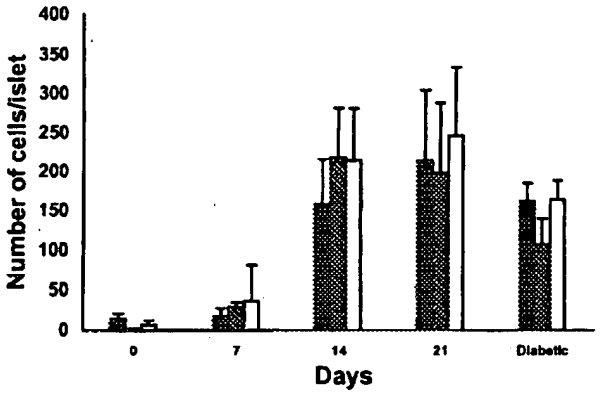

Figure 3. The mean ± SEM number of CD4 cells (solid bars), CD8 cells (hatched bars) and macrophages (open bars) per islet of recipient mice at various time-points following administration of diabetic spleen cells. Immune cell numbers were analyzed from three mice at each time-point. Polynomial regression analyses showed that there was a significant increase in the mean number of each immune cell-type per islet from days 7 to 14 ($p = 0.001$) followed by a slight decline from day 21 to onset of diabetes ($p = 0.01$).

the enzyme was observed in almost all islets with insulitis (Figure 4e–j). Dual-labelling showed that iNOS was co-localized in a proportion of macrophages (Figure 4f,g,h–j). Macrophages positive for iNOS were observed both in the peri-islet and intra-islet locations either as several clusters or occasionally singly. The expression of iNOS was not observed in islets with minimum and peri-islet distributed macrophages or in the exocrine region. Beta cells were devoid of iNOS immunolabelling.

Expression and co-localization of IL-4

Weak IL-4 expressing cells were first observed at days 7 and 14 in a proportion of islets with insulitis (Figure 5a). At day 21, IL-4 expressing cells with weak, moderate and strong immunolabelling were observed within the intra-islet areas (Figure 5b). The immunolabelling became more intense at onset of diabetes (Figure 5c–f). The cytoplasmic staining for the cytokine was usually eccentric and punctate (Figure 5e). Dual-staining showed that IL-4 immunolabelling was confined to mostly CD4 cells, although a proportion of them were devoid of IL-4 immunoreactivity (Figure 5c–f).

Dual staining of pancreatic sections with anti-insulin and anti-IL-4 demonstrated the absence of IL-4 in beta cells (results not shown).

Expression and co-localization of IFN-γ

Immunolabelling for IFN-γ in the periphery of some islets and in exocrine areas was first observed at day 14 (Figure 5g). At day 21 intra-islet areas also began to express the cytokine (Figure 5h). Strong immunolabelling of IFN-γ in intra-islet immune cells was observed at onset of diabetes. The cytoplasmic distribution of the cytokine was punctate and eccentric (Figure 5i–l). Dual labelling showed that intra-islet IFN-γ expressing cells corresponded to mostly macrophages (Figure 5i–l).

Immunolabelling for IFN-γ was also observed in numerous cells located in the exocrine region during the study period. Dual staining showed that the exocrine cells containing the cytokine corresponded to endothelial cells. However, this labelling was not specific to the adoptive transfer model, since endothelial cell immunostaining for the cytokine was also observed in exocrine cells of the pancreas of normal Swiss and Balb/c mice (Figure 5m).

Immunohistochemical controls

In the immunohistochemical procedure for IL-4 or IFN-γ, immunoreactive cells were not observed when the primary antiserum was replaced with PBS, normal rabbit IgG or normal sera from a variety of mammalian species. The use of species incompatible secondary antibodies resulted in an absence of staining. In the dual staining procedure for cytokines and immune cells or cytokines and insulin, omission of one of the primary antisera did not result in immunostaining of the antibody-devoid antigen. When the primary antibodies against IL-4 and IFN-γ were preabsorbed with the corresponding antigens, immunostaining was either absent or reduced considerably. Immunolabelling for insulin, glucagon and somatostatin was absent when the primary antiserum was replaced with normal serum from the immunizing species.

Discussion

The adoptive transfer model has been employed extensively to gain insights on the role of cell-mediated mechanisms underlying various disease intervention measures in the NOD mouse (Tisch *et al.* 1994, Mathieu *et al.* 1995, Harrison *et al.* 1996, Nicoletti *et al.* 1996). Here we have examined this model to establish temporal relationships between intra-islet influx of immune cells and the production of some of the

insulitis (arrowheads) and an islet in (c) without insulitis. (d): Day 14: an islet with insulitis (arrowheads). (e): Day 21: an islet with almost total intra-islet infiltration (arrowheads). (f): Onset of diabetes: an islet with almost total intra-islet infiltration. Scale bars: 1 cm = 60 μm (a–f). (g–r): Representative photomicrographs of pancreatic sections from recipient mice at various time-points following transfer of diabetic spleen cells, showing islets stained by immunofluorescence for CD4 and CD8 cells and macrophages. (g–i): Three serial sections at day 14 showing the distribution of CD4 cells (g), CD8 cells (h) and macrophages (i) within the same islet. (j–l): Three serial sections at day 21 showing the distribution of CD4 cells (j), CD8 cells (k) and macrophages (l) within the same islet. Arrowheads in (j–l) point to the presence of the three cell-types in the exocrine region. (m–o): Three serial sections at day 21 showing the distribution of CD4 cells (m), CD8 cells (n) and macrophages (o) within the same islet. In (o) note that macrophages are distributed as a prominent band within the periphery of the islet. (p–r): Three separate islets from a diabetic mouse showing the distribution of CD4 cells (p), CD8 cells (q) and macrophages (r). Note that all three islets show advanced intra-islet infiltration consisting of the three cell-types. Scale bars: 1 cm = 60 μm (g–l).

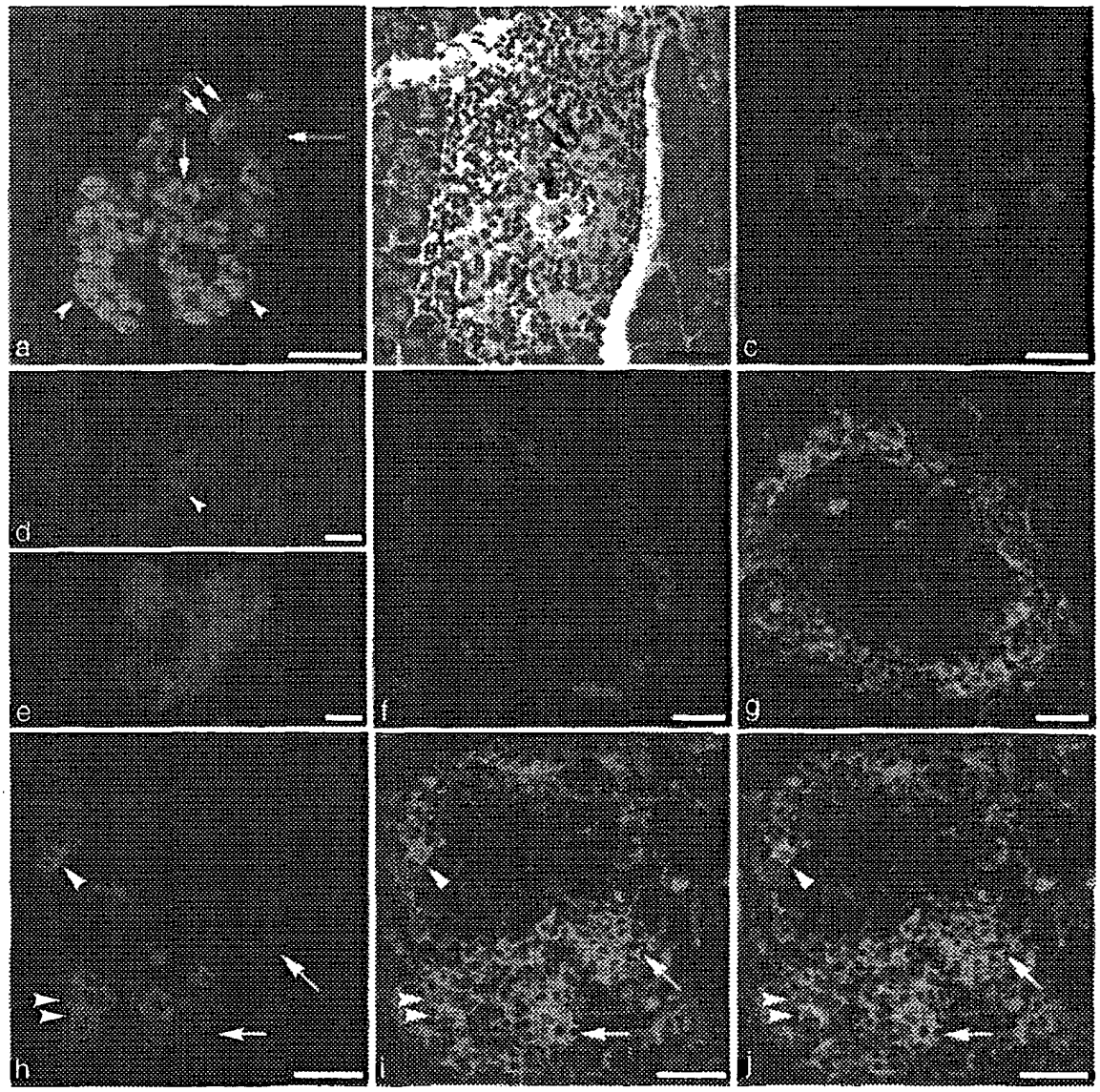

Figure 4. (a–c): Islets from a diabetic mouse showing the distribution of insulin, glucagon and immune cells. (a,b): Confocal view of an islet (a) from a diabetic mouse dual-labelled for insulin (green) and glucagon (red). Note loss of many beta cells in (a). Arrowheads point to well-preserved insulin in beta cells while the arrow with the longer tail points to beta cells weakly stained for insulin. (b) is the same islet subsequently stained by H&E. Arrows in (b) point to the same beta cells denoted by arrows with the shorter tails in (a). Note that the H&E-stained islet shows advanced insulitis. (c): Confocal view of an atrophied islet from the same section as in (a) and (b) stained for glucagon. Note that in the atrophied islet, glucagon cells are re-distributed as a dense core. (d–j): Immunolabelling for iNOS and its co-localization at various time-points following diabetic spleen cell transfer. (d) and (e) are light micrographs while (f)–(j) are confocal views. (d): Day 7: an islet with a few iNOS positive cells (arrowhead). (e–g): Day 14. (e) An islet with strong intra-islet labelling for iNOS. (f) an islet with predominant distribution of iNOS in peripheral areas. (g) is the same islet as in (f) dual-labelled for macrophages (green) and iNOS (red). Note presence of iNOS in selective macrophages (yellow). (h–j): day 21. (h) iNOS labelling in an islet. (i) same islet as in (h) immunolabelled for macrophages. (j) merged view of (h) and (i). Note co-localization of iNOS in selective macrophages. Arrowheads in (h–j) point to strong immunolabelling of iNOS in macrophages while arrows point to weak immunolabelling of iNOS in macrophages. Scale bars: 1 cm = 33 μm (a,f,g–j); 1 cm = 20 μm (b,c); 1 cm = 30 μm (d,e).

putative beta cell inhibitory and protective molecules following cell transfer.

Here we show that transfer of diabetic splenocytes results in significant infiltration of islets from day 14 and is maintained until the onset of diabetes. However, several days elapse between the onset of advanced insulitis and clinical diabetes. The trend in the insulitis scores closely mirrored the increase in the number of intra-islet CD4 and CD8 cells and macrophages. Although islet-located macrophages have been implicated as the earliest immune cells which infiltrate the islets during spontaneous diabetes in the NOD mouse (three weeks), in the low-dose streptozotocin mouse model

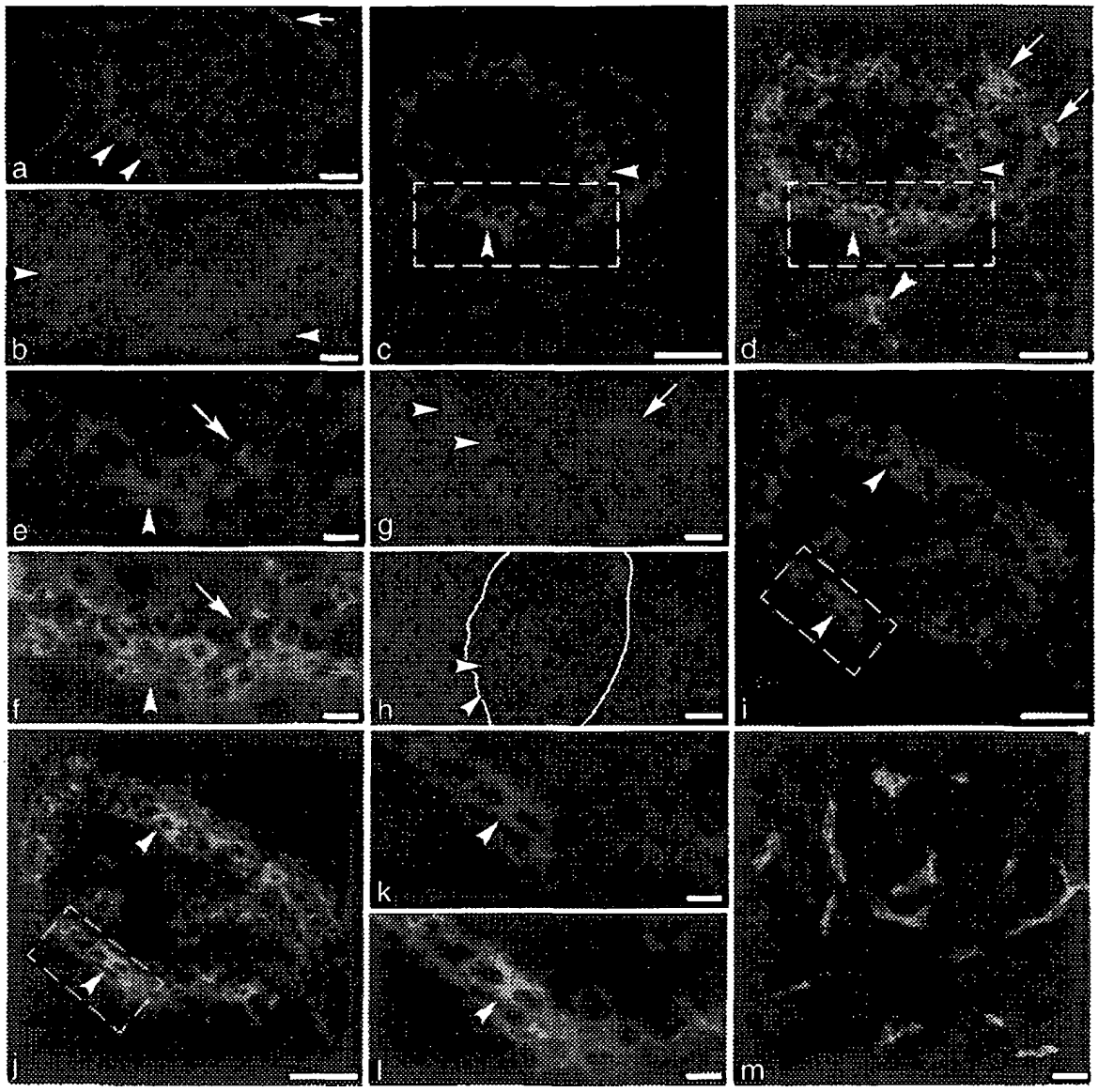

Figure 5. Immunofluorescence photomicrographs of islets or exocrine areas in pancreatic sections of recipient mice and immunostained for IL-4 and IFN-γ (red) and immune or endothelial cells (green). All photomicrographs are confocal images except (a,b,g) and (h) which are light micrographs. (a–f): IL-4 immunolabelling. (a): Day 7. Arrowheads point to IL-4 cells in the periphery of an islet while an arrow points to cells immediately outside the islet. (b): Day 21. Only a part of the islet is shown. Numerous IL-4 positive cells are seen within the islet (arrowheads). (c–f): Diabetic mouse. (c) shows an islet with strong (arrowheads), moderate and weak immunolabelling for IL-4. (d) is a merged view of the same islet dual-labelled for IL-4 (red) and CD4 cells (green). Smaller arrowheads point to CD4 cells expressing IL-4 while arrows point to intra-islet CD4 cells devoid of IL-4. The larger arrowhead points to a CD4 cell outside the islet and which are devoid of IL-4. (e,f): Detailed confocal view of the rectangular area in (c) and (d) showing IL-4 immunolabelling. Arrowheads in (e) and (f) point to the same CD4 cells immunolabelled for IL-4. Note punctate IL-4 immunolabelling in the cytoplasm. Arrows in (e) and (f) point to a CD4 cell with eccentric IL-4 immunolabelling. (g–m): IFN-γ immunolabelling. (g): Day 14. Arrowheads point to IFN-γ immunolabelling in the peripheral cells of a small islet while an arrow points to immunolabelling in some cells in the exocrine area. (h): Day 21. Arrowheads point to IFN-γ immunolabelling in cells within an islet (majority of the islet area is enclosed between the two solid white lines). (i,j): Diabetic mouse. (i) shows an islet with numerous strong (arrowheads), moderate and weak immunolabelling for IFN-γ. (j) is a merged view of the same islet dual-labelled for IFN-γ (red) and macrophages (green). Arrowheads point to macrophages expressing IFN-γ. (k,l): Detailed confocal view of the rectangular area in (i) and (j) showing IFN-γ immunolabelling. Arrowheads in (k) and (l) point to the same macrophages containing IFN-γ. Note eccentric immunolabelling for IFN-γ in the cytoplasm. (m): Merged view of immunolabelling for IFN-γ and endothelial cells in the exocrine pancreas of a normal Swiss mouse. Note co-localization of the cytokine in endothelial cells (yellow). Scale bars: 1 cm = 30 μm (a,b,g,h); 1 cm = 33 μm (c,d,i,j); 1 cm = 17 μm (e,f,k–m).

(five days after the fifth streptozotocin injection) and in the adoptive transfer model (second week after cell transfer), we did not observe their numerical predominance at day 7 (Kolb-Bachoven *et al.* 1988, Hutchings *et al.* 1990, O'Reilly *et al.* 1994). Our results show that at this stage all three cell-types co-existed in approximately equal numbers, usually in the peri-islet areas. At the later stages of prediabetes macrophages were seen in considerable numbers in intra-islet areas in association with T cells.

Advanced insulitis from day 14 was coincident with a marked increase in the expression of iNOS and the two opposing cytokines, IL-4 and IFN-γ within the islet area. Macrophages within the islet are thought to release various cytokines, such as IL-1β and/or IFN-γ (Mandrup-Poulsen *et al.* 1989, Rabinovitch 1993). Cytokine production within the islet macrophage may lead to local NO production following transcription and translation of iNOS (Cetkovic-Cvrlje & Eizirik 1994). Our results concur with a previous study in which islets isolated from mice following adoptive transfer also released increasing levels of NO during the second half of the prediabetic stage (Corbett *et al.* 1993). This period coincided with a parallel impairment of glucose-induced insulin release which suggests that, in this model, NO originating from the islet may be directly toxic to beta cells. In the cyclophosphamide model of accelerated diabetes, an enhanced expression of iNOS in selective macrophages and in association with advanced insulitis are also observed prior to diabetes (Reddy *et al.* 1999).

We show that iNOS labelling is present in selective macrophages and during massive infiltration of islets and rapid beta cell destruction. These studies are in accord with previous findings in the NOD mouse which suggest that intra-islet IL-1β may be insufficient to induce beta cell expression of iNOS (Welsh *et al.* 1995). Transcription and translation of the enzyme in macrophages may be through paracrine or autocrine signals by locally produced IL-1β. Systemically administered IL-1β, either given alone or in combination with IFN-γ and/or TNF-α to NOD mice, results in a similar selective expression of iNOS in macrophages (Reddy *et al.* 1997). However, unlike in the cyclophosphamide model and in the cytokine-treated mice, iNOS expression in beta cells was not observed in the adoptive transfer model despite active beta cell destruction. The possibility that iNOS may be present in some beta cells but at a level beyond the sensitivity of the present immunohistochemical procedure cannot be ruled out completely. More sensitive procedures such as *in situ* reverse transcriptase-PCR and other methods of detecting iNOS protein are necessary to resolve this question.

Immunolabelling of IL-4 was observed in increasing numbers within the islets, at day 21 and persisted at onset of diabetes. The presence of IL-4 cells in the exocrine region, including the perivascular spaces suggest that some immune cells express IL-4 prior to invading the islets. Extra-islet IL-4 induction may occur through several processes including activation of tissue resident mast cells, of natural killer T cells and antigen traffic back to the vascular poles for *de-novo* activation *in situ*. The cytokine was co-localized in a proportion of CD4 cells which also showed varying intensities of immunolabelling. Subpopulations of intra-islet CD4 cells may exist since splenocytes positive for CD45RB^{low}CD4 cells upon stimulation with anti-CD3 produce IL-4 (Shimada *et al.* 1996). The co-localization of IL-4 in CD4 cells is consistent with previous results in other experimental systems (Mossmann & Coffman 1989).

The expression of IFN-γ within the intra-islet areas was observed at day 21 and more strongly at onset of diabetes but in parallel with IL-4 and iNOS expression. However, intra-islet expression of IFN-γ was first detectable after that of IL-4 and iNOS and was co-localized in macrophages. Immunohistochemical analyses of isolated immune cells from syngeneic islet grafts transplanted under the kidney capsule of NOD mice show co-localization of the cytokine in both CD4 and CD8 cells (Suarez-Pinson *et al.* 1996). However, in these studies macrophages were not examined for the presence of IFN-γ. By immunohistochemistry, IFN-γ was reported to be present in lymphocytes of inflamed islets of IDDM patients (Foulis *et al.* 1991). Another cytokine, interferon-α (IFN-α), has been detected at the mRNA level in islets of mice prior to administration of streptozotocin and in BB rats preceding insulitis (Huang *et al.* 1994). It has also been detected in beta cells of human subjects with IDDM and the corresponding mRNA has been found to be elevated in the pancreas of recently diagnosed IDDM subjects (Foulis *et al.* 1987, Huang *et al.* 1995).

In this study, immunoreactive IFN-γ was also observed in a proportion of endothelial cells located in the exocrine areas. The significance of endothelial IFN-γ is unclear since a similar pattern of expression was also observed in pancreatic sections of normal CD-1 and Balb/c mice. However, studies indicate that the endothelium can be a source of several cytokines, including IL-8, a chemotactic cytokine (Kilgore *et al.* 1997).

Recent studies have shown that murine bone marrow-derived macrophages secrete large amounts of IFN-γ protein upon combined stimulation with IL-12 and IL-18 (Munder *et al.* 1998). Macrophages can also be induced to produce IFN-γ upon stimulation with lipopolysaccharide and in mice during pulmonary infection with *Mycobacterium bovis* bacilli Calmette-Guérin (BCG) (Fultzz *et al.* 1993, Wang *et al.* 1999). It is now known that immune cells within the islets of the NOD mouse contain significant amounts of IL-12 and IL-18 mRNA (Rabinovitch *et al.* 1996, Rabinovitch 1998). Therefore, IL-12 and IL-18 may act synergistically and provide a powerful autocrine stimulus for IFN-γ production in macrophages of the NOD mouse. Thus, our present findings indicating macrophages as an important cellular source of IFN-γ may be genuine. By reverse transcriptase-PCR, IFN-γ mRNA can be detected in the pancreas or isolated islets during spontaneous diabetes in the NOD mouse (Rabinovitch *et al.* 1995, Faulkner-Jones *et al.* 1996). However in such studies expression of IFN-γ at the protein level requires verification since post-translational control mechanisms for cytokines are known to exist (Lindsten *et al.* 1989). In other immunohistochemical studies, immune cells isolated from the islets of the

NOD mouse at various stages of the disease did not express this cytokine (Pilstrom *et al.* 1997). In NOD mice where the gene for this cytokine has been deleted, insulitis and diabetes persist, albeit with a delayed onset of the disease (Hultgren *et al.* 1996). Administration of IFN-α inhibits diabetes in the NOD mouse (Sobel & Ahvazi, 1998). In view of these paradoxical findings, the role of IFN-γ in provoking diabetes in the NOD mouse requires further studies.

By *in situ* hybridization, intra-islet expression of genes encoding TNF-α and granzyme A have been demonstrated during spontaneous diabetes in the NOD mouse and subsequently in an adoptive transfer model employing newborn mice as recipients (Held *et al.* 1990, Mueller *et al.* 1995). In the adoptive transfer study, a marked increase in the number of mRNA cells for granzyme A and TNF-α was observed just before the onset of diabetes and in association with increasing insulitis (Mueller *et al.* 1995). In these studies the cellular sources of TNF-α and granzyme A were thought to be CD4 cells and CD8 cells, respectively.

In conclusion, this study shows that in the adoptive transfer model, there is a close temporal relationship between the heightened influx of intra-islet immune cells and the expression of putative beta cell inhibitory molecules such as NO and IFN-γ and clinical diabetes. However, the marked co-expression of IL-4, a putative beta cell protective cytokine at onset of diabetes does not suggest a clear intra-islet Th1 dominance. Further studies are required to identify additional Th1 and Th2 cytokines, their dynamics and cross regulation within the inflamed islets. These studies may contribute to a better understanding of the molecular mechanisms underlying cytokine-induced beta cell destruction or protection during autoimmune diabetes.

Acknowledgements

Financial assistance from the Auckland Medical Research Foundation, National Child Health Research Foundation and the New Zealand Lottery Board is gratefully acknowledged. We are grateful to Dr. C. Nathan for advice regarding the immunohistochemical specificity of anti-iNOS used in this study. We thank Ms. E. Robinson for the statistical analysis.

References cited

Bach JF (1994) Insulin-dependent diabetes mellitus as an autoimmune disease. *Endocr Rev* **15**: 516–542.

Bendelac A, Carnaud C, Boitard C, Bach JF (1987) Syngeneic transfer of autoimmune diabetes from diabetic NOD mice to healthy neonates: requirement for both L3T4$^+$ and Lyt-2$^+$ cells. *J Exp Med* **166**: 823–832.

Cetkovic-Cvrlje M, Eizirik DL (1994) TNF-α and IFN-γ potentiate the deleterious effects of IL-1β on mouse pancreatic islets mainly via generation of nitric oxide. *Cytokine* **6**: 399–406.

Charlton B, Bacelj A, Mandel TE (1988) Administration of silica particles or anti-Lyt 2 antibody prevents β-cell destruction in NOD mice given cyclophosphamide. *Diabetes* **37**: 930–935.

Corbett JA, Mikhael A, Shimizu J, Frederick K, Misko TP, McDaniel ML, Kanagawa O, Unanue ER (1993) Nitric oxide production in islets from nonobese diabetic mice: aminoguanidine-sensitive and -resistant stages in the immunological diabetic process. *Proc Natl Acad Sci USA* **90**: 8992–8995.

Eisenbarth GS, Connelly J, Soeldner JS (1987) The 'natural' history of type I diabetes. *Diabetes Metab Rev* **3**: 873–891.

Faulkner-Jones BE, Dempsey-Collier M, Mandel TE, Harrison LC (1996) Both TH1 and TH2 cytokine mRNAs are expressed in the NOD mouse pancreas *in vivo*. *Autoimmunity* **23**: 99–110.

Foulis AK, Farquharson MA, Meager A (1987) Immunoreactive α-interferon in insulin-secreting β cells in type I diabetes mellitus. *Lancet* **2**: 1423–1427.

Foulis AK, Mcgill M, Farquharson MA (1991) Insulitis in type I (insulin-dependent) diabetes mellitus in man – macrophages, lymphocytes, and interferon-γ containing cells. *J Histopathol* **165**: 97–103.

Fultz MJ, Barber SA, Dieffenbach CW, Vogel SN (1993) Induction of IFN-γ in macrophages by lipopolysaccharide. *Int Immunol* **5**: 1383–1392.

Griffiths GM, Mueller C (1991) Expression of perforin and granzymes *in vivo*: Potential diagnostic markers for activated cytotoxic cells. *Immunology Today* **12**: 415–419.

Harada M, Makino S (1984) Promotion of spontaneous diabetes in non-obese diabetic-prone mice by cyclophosphamide. *Diabetolgia* **27**: 604–606.

Harrison LC, Dempsey-Collier M, Kramer DR, Takahashi K (1996) Aerosol insulin induces regulatory CD8 $\gamma\delta$ T cells that prevent murine insulin-dependent diabetes. *J Exp Med* **184**: 2167–2174.

Held W, MacDonald HR, Weissman IL, Hess MW, Mueller C (1990) Genes encoding tumour necrosis factor alpha and granzyme A are expressed during development of autoimmune diabetes. *Proc Natl Acad Sci USA* **87**: 2239–2243.

Huang X, Hultgren B, Dybdal N, Stewart TA (1994) Islet expression of interferon-α precedes diabetes in both the BB rat and streptozotocin-treated mice. *Immunity* **1**: 469–478.

Huang X, Yuan J, Goddard A, Foulis A, James RFL, Lernmark A, Pujol-Borrell R, Rabinovitch A, Somoza N, Stewart TA (1995) Interferon expression in the pancreases of patients with type I diabetes. *Diabetes* **44**: 658–664.

Hultgren B, Huang X, Dybdal N, Stewart TA (1996) Genetic absence of γ-inteferon delays but does not prevent diabetes in NOD mice. *Diabetes* **45**: 812–817.

Hutchings P, Rosen H, O'Reilly L, Simpson E, Gordon S, Cooke A (1990) Transfer of diabetes in mice prevented by blockade of adhesion-promoting receptor on macrophages. *Nature* **348**: 639–642.

Jansen A, Homo-Delarche F, Hooijkaas H, Leenen PJ, Dardenne M, Drexhage HA (1994) Immunohistochemical characterization of monocytes-macrophages and dendritic cells involved in the initiation of the insulitis and β-cell destruction in NOD mice. *Diabetes* **43**: 667–675.

Kay TWH, Campbell IL, Harrison LC (1991) Characterization of pancreatic T lymphocytes associated with beta cell destruction in the non-obese diabetic (NOD) mouse. *J Autoimmun* **4**: 263–276.

Kikutani H, Makino S (1992) The murine autoimmune diabetes model: NOD and related strains. *Adv Immunol* **51**: 285–322.

Kilgore KS, Schmid E, Shanley TP, Flory CM, Maheshwari V, Tramontini NL, Cohen H, Ward PA, Friedl HP, Warren JS (1997) Sublytic concentrations of the membrane attack complex of complement induce endothelial interleukin-8 and monocyte chemoattractant protein-1 through nuclear factor-κB activation. *Am J Pathol* **150**: 2019–2031.

Kleemann R, Rothe H, Kolb-Bachofen V, Xie Q-W, Nathan C, Martin S, Kolb H (1993) Transcription and translation of inducible nitric oxide synthase in the pancreas of prediabetic BB rats. *FEBS Lett* **328**: 9–12.

Kolb-Bachofen V, Epstein S, Kiesel U, Kolb H (1988) Low dose streptozotocin-induced diabetes in mice. Electron microscopy reveals single-cell insulitis before diabetes onset. *Diabetes* **37**: 21–27.

Lindsten T, June CH, Ledbetter JA, Stella G, Thompson CB (1989) Regulation of lymphokine mRNA stability by a surface mediated T cell activation pathway. *Science* **244**: 339–343.

Mandrup-Poulsen T, Helqvist S, Molvig J, Wogensen LD, Nerup J (1989) Cytokines as immune effector molecules in autoimmune endocrine diseases with special reference to insulin-dependent diabetes mellitus. *Autoimmunity* **4**: 191–218.

Mathieu C, Waer M, Casteels K, Laureys J, Bouillon R (1995) Prevention of type 1 diabetes in NOD mice by nonhypercalcemic doses of a new structural analog of 1,25-dihydroxyvitamin D_3, KH1060. *Endocrinology* **136**: 866–872.

Mossmann TR, Coffman RL (1989) TH1 and TH2 cells: Different patterns of lymphokine secretion lead to different functional properties. *Ann Rev Immunol* **7**: 145–173.

Mueller C, Held W, Imboden MA, Carnaud C (1995) Accelerated β-cell destruction in adoptively transferred autoimmune diabetes correlates with an increased expression of the genes coding for TNF-α and granzyme A in the intra-islet infiltrates. *Diabetes* **44**: 112–117.

Munder M, Mallo M, Eichmann K, Modolell M (1998) Murine macrophages secrete interferon γ upon combined stimulation with interleukin (IL)-12 and IL-18: A novel pathway of autocrine macrophage activation. *J Exp Med* **187**: 2103–2108.

Nicoletti F, Zaccone P, Di Marco R, Di Mauro M, Magro G, Grasso S, Mughini L, Meroni P, Garotta G (1996) The effects of a non-immunogenic form of murine soluble interferon-γ receptor on the development of autoimmune diabetes in the NOD mouse. *Endocrinology* **137**: 5567–5575.

O'Reilly LA, Hutchings PR, Crocker PR, Simpson E, Lund T, Kioussis D, Takei F, Baird J, Cooke A (1991) Characterization of pancreatic islet cell infiltrates in NOD mice: Effect of cell transfer and transgene expression. *Eur J Immunol* **21**: 1171–1180.

Pilstrom B, Bjork L, Bohme J (1997) Monokine-producing cells predominate in the recruitment phase of NOD insulitis while cells producing Th1-type cytokines characterize the effector phase. *J Autoimmun* **10**: 147–155.

Rabinovitch A (1993) Roles of cytokines in IDDM pathogenesis and islet β-cell destruction. *Diabetes Rev* **1**: 215–240.

Rabinovitch A (1998) An update on cytokines in the pathogenesis of insulin-dependent diabetes mellitus. *Diabetes/Metab Rev* **14**: 129–151.

Rabinovitch A, Suarez-Pinson WL, Sorensen O, Bleackley RC, Power RF (1995) IFN-γ gene expression in pancreatic islet-infiltrating mononuclear cells correlates with autoimmune diabetes in non-obese diabetic mice. *J Immunol* **154**: 4874–4882.

Rabinovitch A, Suarez-Pinson WL, Sorensen O (1996) Interleukin 12 mRNA expression in islets correlates with β-cell destruction in NOD mice. *J Autoimmun* **9**: 645–651.

Reddy S, Bibby NJ, Elliott RB (1988a) Ontogeny of islet cell antibodies, insulin autoantibodies and insulitis in the non-obese diabetic mouse. *Diabetologia* **31**: 322–328.

Reddy S, Bibby NJ, Elliott RB (1988b) An immunofluorescent study of insulin-, glucagon-, pancreatic polypeptide- and somatostatin-containing cells in the early ovine fetal pancreas. *Quart J Exp Physiol* **73**: 225–232.

Reddy S, Bibby NJ, Elliott RB (1991) Time course of immune markers in the NOD mouse: Comparison between sexes and animals on an anti-diabetogenic diet. *Diabetes Nutr & Metab Clin and Exp* **4**: 259–265.

Reddy S, Wu D, Swinney C, Elliott RB (1995) Immunohistochemical analyses of pancreatic macrophages and CD4 and CD8 T cell subsets prior to and following diabetes in the NOD mouse. *Pancreas* **11**: 16–25.

Reddy S, Kaill S, Poole CA, Ross J (1997) Inducible nitric oxide synthase in pancreatic islets of the non-obese diabetic mouse: A light and confocal microscopical study of its ontogeny, co-localization and up-regulation following cytokine administration. *Histochemical J* **29**: 53–64.

Reddy S, Yip S, Karanam M, Poole CA, Ross JM (1999) An immunohistochemical study of macrophage influx and the co-localization of inducible nitric oxide synthase in the pancreas of non-obese diabetic (NOD) mice during disease acceleration with cyclophosphamide. *Histochemical J* **31**: 303–314.

Rothe H, Faust A, Schade, U, Kleemann R, Bosse G, Hibino T, Martin S, Kolb H (1994) Cyclophosphamide treatment of female non-obese diabetic mice causes enhanced expression of inducible nitric oxide synthase and interferon-gamma, but not of interleukin-4. *Diabetologia* **37**: 1154–1158.

Shimada, A, Charlton B, Taylor-Edwards C, Fathman CG (1996) β-cell destruction may be a late consequence of the autoimmune process in non-obese diabetic mice. *Diabetes* **45**: 1063–1067.

Signore A, Pozzilli P, Gale EAM, Andreani D, Beverley PCL (1989) The natural history of lymphocyte subsets infiltrating the pancreas of NOD mice. *Diabetologia* **32**: 282–289.

Sobel DO, Ahvazi B (1998) α-Interferon inhibits the development of diabetes in NOD mice. *Diabetes* **47**: 1867–1872.

Suarez-Pinson W, Rajotte RV, Mosmann TR, Rabinovitch A (1996) Both $CD4^+$ and $CD8^+$ T-cells in syngeneic islet grafts in NOD mice produce interferon-γ during β-cell destruction. *Diabetes* **45**: 1350–1357.

Tisch R, Yang XD, Liblau RS, McDevitt HO (1994) Administering glutamic acid decarboxylase to NOD mice prevents diabetes. *J Autoimmun* **7**: 845–850.

Vecchi A, Garlanda C, Lampugnani MG, Resnati M, Matteuccci C, Stoppacciaro A, Schnurch H, Risau W, Ruco L, Mantovani A, Dejana E (1994) Monoclonal antibodies specific for endothelial cells of mouse blood vessels. Their application in the identification of adult and embryonic epithelium. *Eur J Cell Biol* **63**: 247–254.

Wang J, Wakeham J, Harkness R, Xing Z (1999) Macrophages are a significant source of type 1 cytokines during mycobacterial infection. *J Clin Invest* **103**: 1023–1029.

Welsh M, Welsh N, Bendtzen K, Mares J, Strandell E, Oberg C, Sandler S (1995) Comparison of mRNA contents of interleukin-1β and nitric oxide synthase in pancreatic islets isolated from female and male nonobese diabetic mice. *Diabetologia* **38**: 153–160.

Wicker LS, Miller BJ, Mullen Y (1986) Transfer of autoimmune diabetes mellitus with splenocytes from nonobese diabetic (NOD) mice. *Diabetes* **35**: 855–860.

Young LHY, Peterson LB, Wicker LS, Persechini PM, Young JD (1989) *In vivo* expression of perforin by CD8 lymphocytes in autoimmune disease: Studies on spontaneous and adoptively transferred diabetes in nonobese diabetic mice. *J Immunol* **143**: 3994–3999.

Xie Q-W, Cho HJ, Calaycay J, Mumford RA, Swiderek KM, Lee TD, Ding A, Troso T, Nathan C (1992) Cloning and characterization of inducible nitric oxide synthase from mouse macrophages. *Science* **256**: 225–228.